JPET Fast Forward. Published on December 14, 2007 as DOI: 10.1124/jpet.107.131656

JPET #131656

Studies with an Orally Bioavailable α_V Integrin Antagonist in Animal Models of Ocular Vasculopathy: Retinal Neovascularization in Mice and Retinal Vascular Permeability in Diabetic Rats

Rosemary J. Santulli, William A. Kinney, Shyamali Ghosh, Bart L. DeCorte, Li Liu, Robert W. A. Tuman, Zhao Zhou, Norman Huebert, Sven E. Bursell, Alan C. Clermont, Maria B. Grant, Lynn C. Shaw, Shaker A. Mousa, Robert A. Galemmo, Jr., Dana L. Johnson, Bruce E. Maryanoff, and Bruce P. Damiano

Johnson & Johnson Pharmaceutical Research & Development, Welsh and McKean Roads, Spring House, PA 19477-0776 (R.J.S., W.A.K., S.G., B.L.D., L.L., R.W.A.T., Z.Z., N.H., R.A.G. D.L.J., B.E.M., B.P.D.); Neuromed Pharmaceuticals, 301 – 2389 Health Sciences Mall, Vancouver, British Columbia (*R.A.G.); University of Florida, 1600 SW Archer Rd, Gainesville FL 32618 (M.A.G., L.C.S); Pharmaceutical Research Institute at Albany College of Pharmacy, 106 New Scotland Avenue, Albany, NY 12208-3492 (S.A.M); and Beetham Eye Institute, Joslin Diabetes Center, One Joslin Place, Boston, MA 02215 (S.E.B., A.C.C.)*

Running Title: *Oral $\alpha_V\beta_3/\alpha_V\beta_5$ integrin antagonist for ocular vasculopathy*

Corresponding Author:

Rosemary Santulli
Johnson & Johnson Pharmaceutical Research & Development
Welsh and McKean Roads
Spring House, PA 19477-0776
Phone: 215-628-7804
Fax: 215-628-3297
rsantull@prdus.jnj.com

Number of Text pages: 32
Number of Tables: 4
Number of Figures: 6
Number of References: 40
Number of Words in:
Abstract: 200
Introduction: 710
Discussion: 1482

Abbreviations: AMD, age-related macular degeneration; DR, diabetic retinopathy; RGD, arginine-glycine-asparagine; VEGF, vascular endothelial growth factor; FGF, fibroblast growth factor; ROP, retinopathy of prematurity; OIR, oxygen-induced model of retinopathy of prematurity; BSA, bovine serum albumin; DPBS, Dulbecco's phosphate buffered saline; SDS, sodium dodecyl sulfate; HMVEC, human microvascular endothelial cells; HUVEC, human umbilical vein endothelial cells; VEGF-R2, vascular endothelial growth factor receptor type 2; SFM, serum free media; CAM, chick chorioallantoic membrane

Section: Endocrine and Diabetes

Abstract

The α_V integrins are key receptors involved in mediating cell migration and angiogenesis. In age-related macular degeneration (AMD) and diabetic retinopathy (DR), angiogenesis plays a critical role in the loss of vision. These ocular vasculopathies might be treatable with a suitable α_V antagonist, and an oral drug would offer a distinct advantage over current therapies. JNJ-26076713 is a potent, orally bioavailable, nonpeptide α_V antagonist derived from the arginine-glycine-asparagine (RGD) binding motif in the matrix protein ligands (e.g., vitronectin). This compound inhibits $\alpha_V\beta_3$ and $\alpha_V\beta_5$ binding to vitronectin in the low nanomolar range, has excellent selectivity over integrins $\alpha_{IIb}\beta_3$ and $\alpha_5\beta_1$, and prevents adhesion to human, rat, and mouse endothelial cells. JNJ-26076713 blocks cell migration induced by VEGF, FGF, and serum, as well as angiogenesis induced by FGF in the chick chorioallantoic membrane (CAM) model. JNJ-26076713 is the first α_V antagonist reported to inhibit retinal neovascularization in an oxygen-induced model of retinopathy of prematurity (OIR) following oral administration. In diabetic rats, orally administered JNJ-26076713 markedly inhibits retinal vascular permeability, a key early event in diabetic macular edema and AMD. Given this profile, JNJ-26076713 represents a potential therapeutic candidate for the treatment of age-related macular degeneration, macular edema, and proliferative diabetic retinopathy.

INTRODUCTION

Age-related macular degeneration (AMD) is the leading cause of blindness in people over 55 years of age, and diabetic retinopathy (DR) in people under 55 years of age (Klein R., 1994; Williams R., 2004). Both disease conditions are characterized by new blood vessel growth – choroidal neovascularization in the case of AMD and retinal neovascularization in the case of DR (Freund K.L., 1993; Speicher et al., 2003; Williams R., 2004; Zarbin, 2004). There is ample evidence that α_V integrins are involved in ocular angiogenesis. Pro-angiogenic growth factors, including VEGF and FGF, are upregulated in AMD and DR and stimulate α_V expression. In the well-established mouse model of oxygen-induced retinopathy (OIR), or retinopathy of prematurity model (ROP), α_V integrins and the ligand osteopontin are overexpressed in neovascular endothelial cells during the peak time of retinal vessel growth (Takagi et al., 2002). The α_V integrins bind to their extracellular matrix ligands via a specific arginine-glycine-asparagine (RGD) binding site. Cyclic peptides mimicking the RGD binding motif have been developed as potent antagonists to α_V integrins, and when administered via subcutaneous (Friedlander et al., 1996; Chavakis et al., 2002), intraperitoneal, periocular (Luna et al., 1996), or topical (Riecke B., 2001) routes, these cyclic peptides have been shown to inhibit retinal neovascularization in the mouse OIR model. In the laser-induced choroidal neovascularization model (rats), a well-accepted model for AMD, integrins $\alpha_V\beta_3$ and von Willebrand factor are expressed on endothelial cells of new vessels following photocoagulation, but are not expressed in normal choroidal vessels (Kamizuru H., 2001). In this model, intravitreal injection of a cyclic RGD peptide significantly reduced the development of choroidal neovascularization (Yasukawa et al., 2004). Additional evidence has emerged from the use of the extracellular region of brain-specific angiogenesis inhibitor 1 (BAI1-ECR), which is known to exert antiproliferative activity via functional blockade of $\alpha_V\beta_5$ in endothelial cells. Subconjunctival injection of BAI1-ECR (via gene delivery) or an $\alpha_V\beta_5$ antibody showed significantly reduced neovascularization in a rabbit model of laser-induced choroidal neovascularization (Yoon K.C., 2005). In humans, $\alpha_V\beta_3$ and $\alpha_V\beta_5$ are not expressed in normal retinal tissue, but have been observed at elevated levels in vascular cells in the eyes of

patients with DR (Friedlander et al., 1996; Luna et al., 1996), while $\alpha_V\beta_5$ was primarily observed at high levels in ocular tissues in patients with AMD (Friedlander et al., 1996). Increased expression of fibronectin on the inner limiting membrane and $\alpha_V\beta_3$ in the neovessels in eyes of patients with proliferative diabetic retinopathy have also been described (Ljubimov et al., 1996).

Angiogenesis inhibitors targeting VEGF (VEGF aptamer, Macugen, and VEGF monoclonal antibodies) have made a significant impact on the treatment of DR and AMD. A large body of work has been published on the complex relationship between VEGF and α_V integrins. Antagonists of both $\alpha_V\beta_3$ and $\alpha_V\beta_5$ block VEGF-R2 phosphorylation and VEGF-stimulated adhesion, proliferation and migration of endothelial cells (Terai et al., 2001; Tsou and Isik, 2001). Interestingly, in the monkey eye, VEGF induces an angiogenic phenotype in pericytes that accompanies endothelial cells in newly formed vessel sproutings. Correspondingly, in the monkey eye, following exposure to VEGF, $\alpha_V\beta_3$ and $\alpha_V\beta_5$ are highly upregulated in migrating cells from pre-existing and newly formed vessels (Witmer et al., 2004). These studies offer compelling evidence that $\alpha_V\beta_3$ function is necessary for VEGF-mediated effects. Importantly, VEGF and FGF are upregulated in AMD and proliferative DR. Therefore, α_V antagonists may offer broader coverage for these diseases. Furthermore, in both AMD and diabetic retinopathy, VEGF is not only an important angiogenic signal but is also a key regulator of retinal vascular permeability. Vascular permeability involving the breakdown of the blood-retinal barrier is driven by VEGF and is a key element in loss of visual acuity (Patel et al., 2003). While inhibitors of VEGF have been shown to reduce retinal vascular permeability, this effect has not yet been demonstrated with α_V integrin antagonists.

Oral α_V antagonist therapy would represent a novel approach that would be complementary to other treatment modalities, such as VEGF antagonists, which do not affect angiogenesis induced by other growth factors (e.g., FGF) and are not available as oral agents. We report on an orally bioavailable α_V integrin antagonist that markedly inhibits both retinal neovascularization in the retinopathy of prematurity (ROP) model in mice and retinal vascular permeability in diabetic rats.

METHODS

Materials. Integrins $\alpha_v\beta_3$ and $\alpha_v\beta_5$ and Cytomatrix cell adhesion strips were purchased from Chemicon International (Temecula, CA) and anti-human vitronectin IgG rabbit polyclonal antibody from Calbiochem (San Diego, CA). Binding assays were visualized using VectaStain ABC peroxidase kit reagents (Vector Laboratories, Burlingame, CA). Acridine orange and vitronectin were purchased from Sigma-Aldrich Chemical Company (St. Louis, MI). Immulon-2 microtiter plates from Dynatech Laboratories (Chantilly, VA) were used in all binding assays. Human $\alpha_{IIb}\beta_{IIIa}$ from Enzyme Research Laboratories (South Bend, Indiana), human fibrinogen from American Diagnostica, (Greenwich, CT), the biotin-X-NHS biotinylation kit from Calbiochem (San Diego, CA)) were reagents for the $\alpha_{IIb}\beta_{IIIa}$ binding assay. Binding assay plates were read using a microplate reader from Molecular Devices, (Sunnyville, CA). Calcein AM was from InVitrogen (Carlsbad, CA). Adhesions assay plates were read on a Cytofluor 2300 from Millipore (Billerica, MA). Human microvascular endothelial cells (HMVEC) were from Cascade Biologics (Portland, OR), rat endothelial cells from Vec Technologies (Rensselaer, NY), and human umbilical cord endothelial cells (HUVEC) from Cambrex (Charles City, IA). Human K-562 and HT-29 cells were purchased from ATCC (Manassas, VA). Chemotaxis assay plates were from Neuro Probe, (Gaithersburg, MD). JNJ-26076713 (Fig. 1) was synthesized by the methods described in the literature for compound **29d** (Ghosh et al., 2004; Kinney et al., 2007) and used as the HCl salt ($C_{29}H_{38}N_4O_3$ • 2.4HCl • 1.2H_2O). Fresh solutions of the drug were made up daily to minimize cleavage of the central amide or oxidation to the quinoline.

Animals. All animal procedures were in strict accordance with the National Institutes of Health *Guide for the Care and Use of Laboratory Animals* and approved by the University of Florida Institutional Animal Care and Use Committee, Joslin Diabetes Center Animal Care and Use Committee and the Johnson and Johnson Animal Care and Use Committee. Timed pregnant C57BL/6J mice were purchased from Jackson Laboratory (Bar Harbor, Maine) for the ROP model and pharmacokinetic studies. Male Long-Evans rats (Taconic Farms, Germantown, NY) with initial weights between 180 – 250 g were used for the retinal vascular permeability model. All

procedures involving Sprague–Dawley rats from Charles River Laboratories (Wilmington, MA, USA), weighing 250–350 g, were used in the pharmacokinetic studies.

Integrin Binding. Human $\alpha_v\beta_3$ at a concentration of 1 μg/ml dissolved in Tris buffer (20 mM Tris, 1 mM $CaCl_2$, 1 mM $MgCl_2$, 10 μM $MnCl_2$, 150 mM NaCl) was immobilized on Immulon-2 96-well plates overnight at 4 ^oC. Plates were washed and treated with blocking buffer (3% BSA in Tris buffer) for 2 h at 37 ^oC. Plates were then rinsed 2 X in Tris buffer containing 0.3% BSA and 0.2% Tween-20 (assay buffer). Five minutes prior to the addition of 4 nM vitronectin, JNJ-26067613 was added to wells in duplicate. Following a 3-h incubation at 37 ^oC, plates were washed 5 X in assay buffer. An anti-human vitronectin IgG rabbit polyclonal antibody was added and plates were incubated for 1 h at room temperature. VectaStain ABC peroxidase kit reagents employing a biotin labeled anti-rabbit IgG, were utilized for detection of bound antibody. Optical Density (OD) was read at 490 nM on a microplate reader. IC_{50}'s were determined using a 4-parameter-fit logistics model. To determine competition for $\alpha_v\beta_5$ binding, the method was identical to that for human $\alpha_v\beta_3$ except that human $\alpha_v\beta_5$ at a concentration of 1 μg/ml was immobilized on the 96-well plates (Luci et al., 2004). JNJ-26076713 was tested at ½ logarithmic doses from 0.1 – 100 nM in duplicate.

To determine selectivity against $\alpha_{IIb}\beta_{IIIa}$, wells of a 96-well Immulon-2 microtiter plate were coated with 10 μg/ml RGD-affinity purified human $\alpha_{IIb}\beta_{IIIa}$ in 10 mM HEPES, 150 mM NaCl, 1 mM $MgCl_2$ at pH 7.4 (500 ng/well $\alpha_{IIb}\beta_{IIIa}$ final) and incubated overnight at 4 ^oC. The next day, the wells were blocked with 5 % BSA in above buffer at room temperature for 2 h. The assay plate was washed 5 X with modified Tyrode's buffer (150 mM NaCl, 12 mM $NaHCO_3$, 2.6 mM KCl, 2,5 mM Hepes, 1 mM $MgCl_2$, 1 mg/ml BSA, pH 7.4). Biotinylated fibrinogen was prepared using human fibrinogen according to directions from the Biotin-X-NHS Biotinylation Kit. Fifty μl of the compound/ biotinylated fibrinogen mix was transferred to the assay plate and incubated (room temperature) for 2 h. Following incubation, the assay plate was washed (5 X) with modified Tyrode's buffer. Reactions were visualized as described above. JNJ-26076713 was tested at ½ log doses from 0.1 – 30 μM in duplicate.

Cell Adhesion. The ability of JNJ-26076713 to inhibit human, mouse and rat endothelial cell adhesion to vitronectin was evaluated. HMVECs, passage 3 – 9 (Cascade Biologics; Portland, OR), mouse endothelial cells isolated from normal mouse lungs, and rat endothelial cells (Vec Technologies, Inc.; Rensselaer, NY) all at 70–90% confluence were trypsinized from flasks and diluted in Dulbecco's phosphate buffered saline (DPBS) with 0.1% BSA (assay buffer). Cells were labeled with 5 μM Calcein AM in assay buffer for 30 min @ 37 ^{o}C. Cells were washed 3 X in assay buffer. JNJ-26076713 (50 μl) was added at 2 X concentration to each well of the plate containing Cytomatrix vitronectin- coated cell-adhesion strips and tested in duplicate. Labeled endothelial cells (50 μl, 5 X 10^5/ml) were transferred into wells and allowed to adhere for 1 h @ 37 ^{o}C and 5 % CO_2. Plates were washed 3X in assay buffer. Cells were lysed for 15 minutes in 100 μl of 1 M Tris pH 8.0 with 1% SDS. Plates were read at 485 excitation/530 emission (Cytoflour 2300). IC_{50}'s were determined using a four parameter fit logistics model. . JNJ-26076713 was tested at ½ log doses ranging from 0.001 – 1 μM (final concentration in well) in duplicate.

To test for integrin selectivity, the ability of JNJ-26076713 to inhibit K562 cell ($\alpha_5\beta_1$-mediated) adhesion and HT29 cell ($\alpha_V\beta_6$ mediated) adhesion to Cytomatrix® fibronectin-coated adhesion strips was evaluated. The methods were similar to those for endothelial cells. The compound was initially tested in duplicate at 0.1, 0.3, 1, 3, 10, and 50 μM in duplicate in all adhesion assays. In al cell types but the K562 cells, JNJ-2607613 was ultimately tested at ½ logarithmic doses ranging from 0.001 – 3 μM in duplicate.

Cell Migration. FGF, serum and VEGF-induced migration studies are described. For FGF-induced migration, vitronectin (0.4 μg/well) was added to the lower wells of a chemotaxis assay plate. HUVECs, 45 μl of a 2 X 10^6 cells/ml solution and 5 μl of compound was added to wells of a 96 well plate and incubated for 10 min at room temperature. The cell mix (25 μl) and FGF_2 (10 ng/ml) was added to top wells of the holding filter of the chemotaxis assay plate and incubated overnight in cell culture incubator. Media and non-migrated cells were removed from the upper filter (using scraper). The migration filter was washed and fixed in 1.0 % formaldehyde and cell

membranes were permeated with Triton-X-100 (0.2 %) for 15 minutes. The migration filter was then stained with rhodamine phalloidan for 30 min in the dark, washed and air dried prior to measuring fluorescence at 530 excitation/590 emission. All concentrations were run in triplicate and repeated 3 times.

Serum-induced endothelial cell migration assays were performed in 24-Transwell chambers with a polystyrene membrane (6.5 mm diameter, 10 mm thickness, and a pore size of 8 mm). Sub-confluent 24-hr cell cultures (HUVECs) were harvested with trypsin-EDTA, washed twice, and re-suspended in their respective serum free medium (SFM) containing 0.1% BSA. Cells (100,000/500 mL) were added to the upper chamber in the presence or absence of various concentrations of compound. To facilitate chemotactic cell migration, 750 mL of medium containing 2% serum was added to the bottom chambers and the plate, which was placed in a tissue culture incubator. Migration was terminated after 4 to 8 h by removing the cells on the top with a cotton swab and then the filters were fixed with 3% paraformaldehyde and stained with Crystal Violet. The filters were dissolved in 10% acetic acid for 30 minutes. The absorbance was measured at 590 nm. The data were normalized to percent of the vehicle control, which was considered as 100%, and each point is the mean of three transwell filters (+/-SD).

VEGF-induced endothelial cell migration assays were also carried out in 24-Transwell chambers. Briefly, the underside of the membrane was coated with vitronectin (1 mg/mL) for 60 minutes at room temperature, and then blocked with a solution of 1% BSA/PBS at room temperature for 60 minutes. Membranes were washed with PBS and air-dried. Sub-confluent 24-hr cell cultures (HUVECS) were harvested and re-suspended in serum free media containing 0.1% BSA. Cells (100,000/500 mL) containing different concentrations of compound were added to the upper chamber. 750 mL of medium containing 0.1% BSA and 50 ng/mL of VEGF was added to the bottom chambers and the plate was placed in a tissue culture incubator. Migration was terminated after 4 h by removing the cells in the upper chamber with a cotton swab. Filters were treated identically to those in the serum-induced assays. Studies were repeated 3 times. Migration in vitronectin-coated transwell without VEGF stimulation was set as 100%.

JPET Fast Forward. Published on December 14, 2007 as DOI: 10.1124/jpet.107.131656
This article has not been copyedited and formatted. The final version may differ from this version.

All groups were analyzed using Analysis of Variance (ANOVA) followed by un-paired t-tests GraphPad Prism).

Chick Chorioallantoic Membrane Model (CAM). Ten-day old embryos were incubated at 37 ^{o}C with 55% relative humidity. Light was used to define an avascular region, The CAM was dropped and a window, approximately 1.0 cm^2, was cut in the shell over the dropped CAM allowing for direct access to the underlying CAM. FGF_2 was used as a standard pro-angiogenic agent to induce new blood vessel branches on the CAMs of 10-day old chick embryos. Sterile filter disks absorbed with FGF_2 (1 μg/ml) dissolved in PBS were placed on growing CAMs. At 24 hours, JNJ–26076713 was added directly (topically) at 0.1, 1 and 10 μg per CAM (N = 7 per dose). CAM tissue directly beneath the filter disk was resected from embryos treated 48 hours prior with the JNJ-26076713. Tissues were washed 3X with PBS, and examined under a stereomicroscope. Digital images of CAM sections adjacent to filters were collected using a 3-CCD, color video camera system and analyzed with Image-Pro Plus software. The number of vessel branch points contained in a circular region equal to the area of a filter disk was counted for each section (Ribatti et al., 2000).

Pharmacokinetic Studies in Rats and Mice. Rats and mice (N=4) were dosed intravenously (iv) at 2 mg/kg and by oral gavage at 10 mg/kg with JNJ-26076713 formulated in 5% dextrose in water (D5W). Blood samples were collected at 5 (iv only), 15, and 30 min and at 1, 2, 4, 7 and 24 h post-dosing into heparinized (lithium) tubes. Blood samples were centrifuged for cell removal and two 200-μl plasma samples were stored at –70 ^{o}C for later analysis. Blank species-specific plasma was used for preparation of standard curves. Acetonitrile (150 μl) was added to 50 μl of plasma to precipitate proteins. Samples were centrifuged and supernatant removed for analysis by LC-MS-MS. A ratio of three parts acetonitrile to one part plasma was maintained for all studies when <200 μl of plasma was available.

OIR Model. In the mouse model of oxygen-induced retinopathy (Grant M.B., 2004) mice at postnatal day seven were placed with their nursing dams in a 75% oxygen atmosphere for 5 days. Upon return to normal air, these mice develop retinal neovascularization, with peak development occurring 5 days (P_{17}) after their return to normoxia. On day 12, the mouse pups

received 30, 60 or 120 mg/kg JNJ-26076713 by gavage twice daily for 5 days. Compound solutions were made up fresh in D5W pH 2.0. After the fifth day of treatment (following return to normoxia), the animals were euthanized and the eyes removed and fixed in 4% paraformaldehyde, and then embedded in paraffin. Three hundred serial sections (6 μm) were cut sagitally through the cornea parallel to the optic disc. Every thirtieth section was placed on slides and stained with hematoxylin-eosin (H&E). This resulted in ten sections from each eye being scored in a masked fashion using light microscopy to count endothelial nuclei extending beyond the inner limiting membrane into the vitreous as previously described (Smith et al., 1994). The efficacy of treatment was calculated as the percent average nuclei per section for both eyes comparing treated versus untreated animals. All groups were analyzed using ANOVA followed by Tukey's multiple comparison test (GraphPad Prism). Blood was removed from a subset of mice 12 to 14 hours after the last dose of compound and plasma samples frozen for analyses of drug levels. No samples were taken from the 120 mg/kg dose group.

Diabetes Induced Retinal Vascular Permeability Model. Retinal physiological measurements were performed to investigate whether oral treatment with JNJ-26076713 in a prevention regime affected retinal physiology in 2-week diabetic Long-Evans rats. (Abiko et al., 2002). Treatment was initiated upon confirmation of diabetes after streptozotocin (STZ) injection. Untreated Long-Evans rats served as non-diabetic controls. Forty-eight rats were distributed in 4 groups of 10-12 animals each as follows: nondiabetic rat + vehicle (D5W); nondiabetic rat + JNJ-26076713 (60 mg/kg/, b.i.d.); diabetic rat + vehicle (D5W); diabetic rat + JNJ-26076713 (60 mg/kg/, b.i.d.). Treated rats were administered JNJ-26076713 in D5W (pH 2.0) twice daily (8AM and 5PM) by oral gavage). Control animals were treated in a similar manner using only vehicle. Animal condition was monitored daily. Blood glucose and body weight were monitored. Hematocrit was also tested to insure that animals did not become dehydrated.

On day 13, a jugular vein catheter was surgically implanted. On day 14, rats underwent retinal leukostasis measurements using acridine orange leukocyte fluorography (Abiko et al., 2002). Briefly, acridine orange was infused (750 μl/min) through the jugular vein catheter and after twenty minutes, retinal images from both eyes were obtained to assess static stained

leukocytes. For retinal vascular permeability measurements, rats were infused with Evans Blue on day 15 using a standard in vivo protocol (Xu et al., 2001). Briefly, two hours after Evans Blue perfusion the animals were sacrificed and retinas removed for permeability measurements. The eyes are enucleated and the retinae are carefully dissected away under an operating microscope. The weight of each retina is measured after drying for 4 hours in a Speed-Vac. Albumin leakage into the retinal tissue is estimated via the measurement of extravasated Evans blue dye. Evans blue is extracted by incubating each retina in 0.24 ml of formamide for 18 hours at 72°C. The extract is filtered through a 30,000 MW filter at a speed of 12,000 rpm for 120 minutes at 4°C. The absorbance of the filtrate is measured with a spectrophotometer at 620 nm and 740 nm, the absorption maximum and minimum for Evans blue in formamide. Retinal permeability is expressed as ng Evans Blue/g retina dry weight. An increase in this measurement indicates leakage of Evans blue into the retina and an increase in vascular permeability.

At the time of catheterization, a blood sample was withdrawn for determination of compound concentration. Group sizes allowed for demonstration of a 25-30% change with a p value < 0.05 at a power of 0.8 using t-test or ANOVA. The retinal physiological response to the treatment was compared to the untreated control groups for both diabetic and non-diabetic rats.

JPET Fast Forward. Published on December 14, 2007 as DOI: 10.1124/jpet.107.131656
This article has not been copyedited and formatted. The final version may differ from this version.

RESULTS

In Vitro Studies. JNJ-26076713 is a potent inhibitor of both human $\alpha_v\beta_3$ and $\alpha_v\beta_5$ binding to vitronectin, demonstrating IC_{50}'s of 2.3 ± 0.27 nM (N = 18) and 6.3 ± 0.83 nM (N = 11), respectively. In contrast, JNJ-26076713 was extremely weak in its ability to inhibit human $\alpha_{IIb}\beta_3$ binding with an IC_{50} of 4690 ± 170 nM (N = 2). Furthermore, JNJ-26076713 was 4.5- and 23-fold more potent respectively in inhibiting human endothelial cell adhesion to vitronectin as compared to rat and mouse endothelial cell adhesion (Table I). This species differentiation is relevant when considering the effects of JNJ-26076713 in mouse and rat in vivo models of efficacy. To further characterize integrin specificity, $\alpha_V\beta_6$ and $\alpha_5\beta_1$ mediated adhesion was evaluated. JNJ-26076713 did not inhibit human $\alpha_5\beta_1$ mediated adhesion while it was moderately active in inhibiting $\alpha_V\beta_6$ mediated adhesion (Table I).

JNJ-26076713 dose-dependently inhibited HUVEC migration to serum. Additionally, JNJ-26076713 was a potent inhibitor of FGF_2 – induced HUVEC migration (Fig. 2A). In experiments in which VEGF was the migration stimulus, VEGF induced HUVEC migration was increased more than 2-fold (222%). As demonstrated in Figure 2, JNJ-26076713 produced concentration-dependent inhibition of HUVEC migration stimulated by VEGF with an IC_{50} of 30 nM. IC_{50} values calculated from the serum and FGF migration studies were 29 and 31 nM, respectively, indicative of the ability of JNJ-26076713 to be a potent inhibitor of endothelial migration induced by a number of physiological factors.

JNJ-26076713 demonstrated potent inhibition of angiogenesis in the CAM model as shown in Figure 3. Even at the lowest dose of JNJ-26076713, 0.1 μg/CAM, a 72% inhibition of FGF-induced angiogenesis was observed. Figure 4 exemplifies the inhibitory effect in this model at both 0.1 and 10 μg/ml of JNJ-26076713. The new vessel growth induced by FGF (Fig. 4B) is nearly eliminated following exposure to either dose of antagonist (Fig. 4C and 4D).

Pharmacokinetics. JNJ-26076713 was administered either intravenously (2 mg/kg) or orally (10 mg/kg) to male rats and plasma compound levels measured. Derived pharmacokinetic parameters are shown in Table 2. Volume of distribution (1100 mL/kg) was slightly larger than rat

total body water (668 mL/kg), suggesting that the compound is well distributed. The clearance was low compared to liver blood flow (55 mL/min/kg), with a resulting terminal elimination$t_{1/2}$ of 10 h. Oral bioavailability was 21%.

Derived pharmacokinetic parameters in mice are shown in Table 3. Plasma concentrations decreased in a biphasic manner after iv administration. JNJ-26076713 had a high volume of distribution in the mouse (5504 mL/kg) compared to mouse total body water of 725 mL/kg, and low clearance (7 mL/min/kg) compared to mouse liver blood flow of 90 ml/min/kg. The $t_{1/2}$ was similar to that in the rat after iv administration but somewhat shorter after oral administration. Oral bioavailability in mice was similar to rats. The pharmacokinetic profile indicated that oral, twice daily dosing would be suitable for adequate drug exposure for *in vivo* efficacy studies in either rats or mice.

In Vivo Disease Models. JNJ-26076713 significantly inhibited retinal neovascularization at all doses tested ($p < 0.001$). Inhibition was dose dependent (Fig. 5) with a 33%, 43% and 67% inhibition of neovascularization at 30, 60 and 120 mg/kg respectively. Drug levels, representing trough levels, were 3.9 and 4.1 μM after the 30 and 60 mg/kg dosing, respectively, indicating excellent exposure levels based on plasma samples 12 to 14 hours after the final oral dose. Blood samples were not taken in the 120 mg/kg dose group.

JNJ-26076713 inhibited the increase in retinal vascular permeability and leukostasis associated with diabetes (Fig. 6). JNJ-26076713, 60 mg/kg, *b.i.d.*, demonstrated significant inhibition of retinal vascular permeability in STZ diabetic rats. Furthermore, JNJ-26076713 treatment tended to reduce leukocyte adhesion (48% reduction representing the decrease in number of static leukocytes in diabetic treated mice from vehicle treated diabetic rats using the non diabetic vehicle treated mice as a baseline), albeit this reduction was not statistically significant. There were no significant changes in body weight or plasma glucose levels associated with JNJ-26076713 treatment as shown in Table 4. Levels of JNJ-26076713 in plasma samples drawn at either 1-3 or 4-6 hours following the last oral dose indicated good compound exposure in both diabetic rats (4.6 ± 0.7 and 7.6 ± 1.0 μM, respectively) and non-diabetic rats (5.3 and 6.4 μM, respectively, from a single sample).

JPET Fast Forward. Published on December 14, 2007 as DOI: 10.1124/jpet.107.131656
This article has not been copyedited and formatted. The final version may differ from this version.

DISCUSSION

This report describes the in vitro and in vivo pharmacological activity of a novel α_V antagonist, JNJ-26076713, which was shown to inhibit both retinal neovascularization in a mouse retinopathy model and retinal vascular permeability increase in diabetic rats when delivered orally. These findings represent the first demonstration of therapeutic activity of an orally delivered α_V integrin antagonist in models of retinopathy. JNJ-26076713 was derived from the RGD binding motif and was optimized to yield a potent antagonist of human $\alpha_V\beta_3/\alpha_V\beta_5$, as demonstrated in both ligand binding assays as well as in cell adhesion and migration assays. Although somewhat less potent in mouse and rat $\alpha_V\beta_3/\alpha_V\beta_5$, its activity was sufficient for assessing efficacy in the retinopathy model in the mouse and the vascular permeability model in the rat. Admittedly, the variability of potency to inhibit endothelial cell adhesion among species was limited to one endothelial type per species and could be attributed to difference in the origin of the endothelial cell. We have not, however, seen significant differences in inhibitory potency of JNJ-26076713 between human endothelial cell and human tumor cell adhesion in those tumor lines that express α_V integrins (data not shown). JNJ-26076713 also had good oral bioavailability and elimination half-life in mice and rats (this report) as well as in dogs and monkeys (data not shown), producing excellent plasma compound exposure and volume of distribution beyond the plasma compartment.

Integrins bind protein ligands that are components of the extracellular matrix, such as collagens, fibronectin, fibrinogen, vitronectin, osteopontin, and laminin. There are specific ligand-binding patterns for each integrin (Hodivala-Dilke, 2003; Mousa, 2003). The α_V integrins are expressed on several cell types including osteoclasts, vascular smooth muscle cells, endothelial cells and a variety of tumor cells (Mousa, 2002). The α_V integrins bind to their extracellular matrix ligands at the RGD binding site. Cyclic peptides and small molecules mimicking this RGD binding motif have been developed as potent antagonists (Eliceiri and Cheresh, 1998; Mousa, 2002; Mousa, 2003; Ruegg and Mariotti, ; Williams R., 2004) and have shown efficacy in animal models of DR, AMD, osteoporosis, restenosis, arthritis, tumor growth and metastasis. Additionally, monoclonal antibodies to these integrins have also been demonstrated to be

JPET Fast Forward. Published on December 14, 2007 as DOI: 10.1124/jpet.107.131656
This article has not been copyedited and formatted. The final version may differ from this version.

efficacious in these models. (Miller et al., 2000; Wilder, 2002; Trikha et al., 2004; Cai and Chen, 2006) Cilengitide, an RGD mimetic peptide, and CNTO 95, a pan α_V monoclonal antibody, are currently in Phase II clinical trials while Vitaxin, an $\alpha_V\beta_3$ monoclonal antibody, is in Phase III trials (The Investigational Drug Database) for treatment of cancer and a variety of solid tumors.

Monoclonal antibodies to α_V integrins and RGD mimetic peptides have demonstrated the capacity to diminish both retinal and choroidal neovascularization in animal models (Luna et al., 1996; Kamizuru H., 2001; Riecke B., 2001; Chavakis et al., 2002; Witmer et al., 2004; Yasukawa et al., 2004; Yoon K.C., 2005). To date, there has been only one published report of a non-peptide α_V small molecule antagonist evaluated in an animal model of DR or AMD. SB-267268, administered intraperitoneally at 60 mg/kg, *b.i.d.*, reduced angiogenesis in the murine OIR model by approximately 50%. Additionally, both VEGF and VEGFR-2 expression in the inner retina was attenuated with SB-267268 (Wilkinson-Berka Jennifer et al., 2006). JNJ-26076713 was shown to produce a similar extent of angiogenesis inhibition in the ROP model, but in contrast to SB-267268, was efficacious following oral dosing. No other small or large molecule α_V antagonist delivered via any route has been shown to inhibit increases in retinal vascular permeability associated with diabetes. Breakdown of the blood retinal barrier is an early characteristic of DR and correlates to vision loss. Vascular permeability and leakage are prevalent in both AMD and DR. JNJ-26076713 was effective in preventing vascular permeability increase in diabetic rats and also tended to decrease leukostasis, although this effect was not statistically significant. Leukostasis can result from insulin resistance prior to the onset and in the absence of diabetes. However, alterations in retinal blood flow and vascular permeability are dependent on the diabetic state and hyperglycemia (Abiko et al., 2002). Therapies that can reduce retinal vascular permeability as well as prevent neovascularization could have improved outcomes in limiting loss of vision.

Concern has existed regarding the safety of long-term systemic administration of α_V antagonists including potential side effects such as inhibition of wound healing. Recent evidence has lessened this concern, since an orally active α_V antagonist L-845704 showed no serious adverse effects after one year of treatment in postmenopausal osteoporotic women (Murphy et

al., 2005). Furthermore, infusions of monoclonal antibodies to $\alpha_V\beta_3$ and/or $\alpha_V\beta_5$, resulting in sustained systemic exposure, did not hinder wound healing in monkeys and man (Martin et al., 2005; Zhang et al., 2007). Current standard of care for retinopathies utilizes intravitreal injection of therapeutics or laser photocoagulation. A safe and orally effective α_V antagonist may provide the means to either sustain or improve outcomes of laser therapy or intravitreal injections of either Macugen or Lucentis and ultimately might limit the need for these more invasive treatments and improve compliance.

The newest therapies for AMD and DR are anti-angiogenic therapies targeting VEGF (Lucentis and Macugen). In part, angiogenesis involves adhesive interaction of endothelial cells with the extracellular matrix. JNJ-26076713 inhibits human, mouse and rat endothelial cell adhesion, however it is several fold less potent in its effects on rat and mouse adhesion. Thus, the doses and plasma compound levels associated with efficacy in the rodent models overestimate the likely effective doses and plasma levels, given the greater potency in inhibiting human endothelial cell adhesion. JNJ-26076713 is also a potent inhibitor of endothelial cell migration induced by FGF, VEGF and serum with nearly identical potencies. This activity may represent an advantage over VEGF therapies alone as treatments for AMD or DR. Growth factors as well as cytokines increase integrin expression and are also key elements in angiogenesis pathways. In the chick CAM, FGF specifically induces β_3 expression while VEGF induces β_5 expression. (Friedlander et al., 1996) Importantly, VEGF, FGF as well as other prominent growth factors such as IGF, which is present in serum, are upregulated in AMD and proliferative diabetic retinopathy (Simo et al., 2006). Ligand occupancy of $\alpha_V\beta_3$ has been reported to be a prerequisite for IGF to induce cell migration and proliferation (Clemmons and Maile, 2005).

JNJ-26076713 exhibited excellent exposure levels in both the mouse and rat models following twice daily oral dosing. In the mouse ROP model, > 1 μM levels were detected even at trough (12 – 14 hours after the final oral dose). Moreover, JNJ-26076713 has been shown to have no adverse activity in animal models of cardiovascular and CNS safety (data not shown) and its selectivity was notable as indicated by lack of significant interaction with a panel of 51

receptors and ion channels and 152 kinases (data not shown). JNJ-26076713 demonstrated some capacity to inhibit $\alpha_V\beta_6$ mediated adhesion. While $\alpha_V\beta_6$ expression is limited to the epithelium, where expression is typically low, it can be highly elevated in carcinomas and in chronic wounds. (Haekkinen et al., 2004; Bates, 2005) Therefore, it is likely that modest inhibition of $\alpha_V\beta_6$ should not affect the overall profile of JNJ-26076713.

Integrin α_V antagonists have been studied for several years and their utility in several disease models have been well documented. Clinically, the most therapeutically active area is oncology. Most recently, there has also been a strong interest in targeting α_V integrins as imaging/targeting agents in cancer. (Lim et al., 2005) Merck successfully demonstrated clinical efficacy for their α_V antagonist in osteoporosis. However, most likely due to successful and less expensive pre-existing therapies, such as Fosamax (alendronate sodium), further development of α_V antagonists for this indication were not pursued.

AMD and DR represent a large unmet medical need and may represent an important new opportunity for α_V antagonists. The α_V antagonist SB-267268 is reported to be in Phase I clinical trials for AMD (www.gsk.com). Inhibiting the leakage in existing blood vessels and preventing abnormal angiogenesis with an orally bioavailable α_V antagonist would represent an excellent therapy for preventing the retinal or choroidal neovascularization associated with DR and AMD.

In conclusion, JNJ-26076713 is the first small-molecule α_V antagonist with oral efficacy in both inhibiting retinal neovascularization in a model of retinopathy as well as retinal vascular permeability increase in a diabetic model. $\alpha_V\beta_3$ and $\alpha_V\beta_5$ integrins in particular have been implicated in retinal neovascularization and are likely the primary targets responsible for the pharmacologic effects of JNJ-26076713 in these models. The potential of α_V antagonists in the treatment of AMD and DR is only beginning to be explored in the clinical setting. The availability of an oral therapeutic agent for the treatment of AMD and DR has the potential to reduce the frequency of the current invasive treatments and improve upon overall outcome. JNJ-26076713 therefore represents a potential therapeutic candidate with the convenience of oral bioavailability

for the treatment of age-related macular degeneration, macular edema, and proliferative diabetic retinopathy.

ACKNOWLEDGMENTS

The authors thank Yanmin Chen and Deping Cheng for bioanalytical and pharmacokinetic analysis; and Andrew Darrow, Claudia Derian, Cailin Chen, and Charles Smith for their technical help and advice throughout this project.

REFERENCES

Abiko T, Abiko A, Clermont AC, Shoelson B, Horio N, Takahashi J, Adamis AP, King GL and Bursell SE (2002) Characterization of retinal leukostasis and hemodynamics in insulin resistance and diabetes. *Diabetes* **52**:829-837.

Bates RC (2005) Colorectal cancer progression; integrin av.b6 and the epithelial-mesenchymal transition (EMT). *Cell Cycle* **4**:1350-1352.

Cai W and Chen X (2006) Anti-angiogenic cancer therapy based on integrin alphavbeta3 antagonism. *Anticancer Agents Med Chem FIELD Full Journal Title:Anti-cancer agents in medicinal chemistry* **6**:407-428.

Chavakis E, Riecke B, Lin J, Linn T, Bretzel RG, Preissner KT, Brownlee M and Hammes HP (2002) Kinetics of integrin expression in the mouse model of proliferative retinopathy and success of secondary intervention with cyclic RGD peptides. *Diabetologia* **45**:262-267. FIELD Reference Number: FIELD Journal Code:0006777 FIELD Call Number:.

Clemmons DR and Maile LA (2005) Interaction between insulin-like growth factor-I receptor and aVb3 integrin linked signaling pathways: Cellular responses to changes in multiple signaling inputs. *Molecular Endocrinology* **19**:1-11.

Eliceiri BP and Cheresh DA (1998) The role of av integrins during angiogenesis. *Molecular Medicine (New York)* **4**:741-750.

Freund K.L. YLSJ (1993) Age-related macular degeneration and choroidal neovascularization. *American Journal of Opthalmology* **115**:786-791.

Friedlander M, Theesfeld CL, Sugita M, Fruttiger M, Thomas MA, Chang S and Cheresh DA (1996) Involvement of integrins alpha v beta 3 and alpha v beta 5 in ocular neovascular diseases. *Proceedings of the National Academy of Sciences of the United States of America* **93**:9764-9769. FIELD Reference Number: FIELD Journal Code:7505876 FIELD Call Number:.

Ghosh S, Santulli RJ, Kinney WA, DeCorte BL, Liu L, Lewis JM, Proost JC, Leo GC, Masucci J, Hageman WE, Thompson AS, Chen I, R. K, Tuman RW, Galemmo RAJ, Johnson DL,

Damiano BP and Maryanoff BE (2004) 1,2,3,4-Tetrahydroquinoline-containing aVb3 integrin antagonists with enhanced oral bioavailability. *Bioorganic & Medicinal Chemistry Letters* **14**:5937-5941.

Grant M.B. AA, Spoerri P., Pan H., Shaw L.C., Mames R.N. (2004) The role of growth factors in the pathogenesis of diabetic retinopathy. *Expert Opinion in Investigational Drugs* **13**:1275-1293.

Haekkinen L, Koivisto L, Gardner H, Saarialho-Kere U, Carroll JM, Lakso M, Rauvala H, Laato M, Heino J and Larjava H (2004) Increased expression of b6-integrin in skin leads to spontaneous development of chronic wounds. *American Journal of Pathology* **164**:229-242.

Hodivala-Dilke KM, Reynolds A.R., Reynolds, L.E. (2003) Integrins in angiogenesis: multitalented molecules in a balancing act. *Cell Tissue Research* **314**:131-144.

Kamizuru H. KH, Yasukawa T., Tabata Y., Honda Y., Ogura Y. (2001) Monoclonal antibody-mediated drug targeting to choroidal neovascularization in the rat. *nvestigative Ophthalmology and Visual science* **42**:2664-2672.

Kinney WA, Teleha C, Thompson AS, Newport M, Hansen R, Ballentine S, Ghosh S, A. Mahan, Grasa G, Zanotti-Gerosa A, Dingenen J, Schubert C, McComsey DF, Leo G, Santulli RJ and Maryanoff BE (2007) Application of a suzuki-miyaura approach to the stereoselective synthesis of a 1,2,3,4-tetrahydroquinoline-containing dual aVb3/aVb5 integrin antagonist.

Klein R. KBE, Moss S.E., Cruickshanks K.J. (1994) The Wisconsin Epidemiologic Study of diabetic retinopathy. XIV. Ten-year incidence and progression of diabetic retinopathy. *Archives of Ophthalmology* **112**:1217-1228.

Lim EH, Danthi N, Bednarski M and Li KCP (2005) A review: Integrin avb3-targeted molecular imaging and therapy in angiogenesis. *Nanomedicine* **1**:110-114.

Ljubimov AV, Burgeson RE, Butkowski RJ, Couchman JR, Zardi L, Ninomiya Y, Sado Y, Huang Z-S, Nesburn AB and Kenney MC (1996) Basement membrane abnormalities in human eyes with diabetic retinopathy. *Journal of Histochemistry and Cytochemistry* **44**:1469-1479.

Luci DK, Santulli RJ, Gauthier DA, Tounge BA, Ghosh S, Proost JC, Kinney WA, De Corte B, Galemmo RA, Jr., Lewis JM, Dorsch WE, Wagaman MW, Damiano BP and Maryanoff BE (2004) A concise synthesis of an indenopyrrolidine-based dual avb3/avb5 integrin antagonist. *Heterocycles* **62**:543-557.

Luna J, Tobe T, Mousa SA, Reilly TM and Campochiaro PA (1996) Antagonists of integrin alpha v beta 3 inhibit retinal neovascularization in a murine model. *Laboratory investigation; a journal of technical methods and pathology* **75**:563-573. FIELD Reference Number: FIELD Journal Code:0376617 FIELD Call Number:.

Martin PL, Jiao Q, Cornacoff J, Hall W, Saville B, Nemeth JA, Schantz A, Mata M, Jang H, Fasanmade AA, Anderson L, Graham MA, Davis HM and Treacy G (2005) Absence of Adverse Effects in Cynomolgus Macaques Treated with CNTO 95, a Fully Human Anti-av Integrin Monoclonal Antibody, Despite Widespread Tissue Binding. *Clinical Cancer Research* **11**:6959-6965.

Miller WH, Keenan RM, Willette RN and Lark MW (2000) Identification and in vivo efficacy of small-molecule antagonists of integrin av.b3 (the vitronectin receptor). *Drug Discovery Today* **5**:397-408.

Mousa SA (2002) Anti-integrin as novel drug-discovery targets: potential therapeutic and diagnostic implications. *Current Opinion in Chemical Biology* **6**:534-541.

Mousa SA (2003) aV vitronectin receptors in vascular-mediated disease. *Medicnal Research Reviews* **23**:190-199.

Murphy MG, Cerchio K, Stoch SA, Gottesdiener K, Wu M and Recker R (2005) Effect of L-000845704, an avb3 integrin antagonist, on markers of bone turnover and bone mineral density in postmenopausal osteoporotic women. *Journal of Clinical Endocrinology and Metabolism* **90**:2022-2028.

Patel N, Sun L, Moshinsky D, Chen H, Leahy K, Le P, Moss KG, Wang X, Rice A, Tam D, Laird AD, Yu X, Zhang Q, Tang C, McMahon G and Howlett A (2003) A selective and oral small molecule inhibitor of vascular epithelial growth factor receptor (VEGFR)-2 and

VEGFR-1 inhibits neovascularization and vascular permeability. *Journal of Pharmacology and Experimental Therapeutics* **306**:838-845.

Ribatti D, Vacca A, Roncali L and Dammacco F (2000) The chick embryo chorioallantoic membrane as a model for in vivo research on anti-angiogenesis. *Current Pharmaceutical Biotechnology* **1**:73-82.

Riecke B. CE, Bretzel R.G., Linn T., Preissner K.T. Brownlee M., Hammes H.-P. (2001) Topical application of integrin antagonists inhibit proliferative retinopathy. *Hormone Metabolism Research* **33**:307-311.

Ruegg C and Mariotti A (2003) Vascular integrins: pleiotropic adhesion and signaling molecules in vascular homeostasis and angiogenesis. *Cellular and molecular life sciences : CMLS* **60**:1135-1157. FIELD Reference Number:1272 FIELD Journal Code:9705402 FIELD Call Number:.

Simo R, Carrasco E, Garcia-Ramirez M and Hernandez C (2006) Angiogenic and antiangiogenic factors in proliferative diabetic retinopathy. *Current Diabetes Reviews* **2**:71-98.

Smith LE, Wesolowski E, McLellan A, Kostyk SK, R. DA, Sullivan R and D'Amore PA (1994) Oxygen-induced retinopathy in the mouse. *Invest Opthalmol Vis Svi* **35**:101-111.

Speicher MA, Danis RP, Criswell M and Pratt L (2003) Pharmacologic therapy for diabetic retinopathy. *Expert Opinion on Emerging Drugs* **8**:239-250.

Takagi H, Suzuma K, Otani A, Oh H, Koyama S, Ohashi H, Watanabe D, Ojima T, Suganami E and Honda Y (2002) Role of Vitronectin Receptor-Type Integrins and Osteopontin in Ischemia-Induced Retinal Neovascularization. *Japanese Journal of Ophthalmology* **46**:270-278.

Terai Y, Abe M, Miyamoto K, Koike M, Yamasaki M, Ueda M, Ueki M and Sato Y (2001) Vascular smooth muscle cell growth-promoting factor/F-spondin inhibits angiogenesis via the blockade of integrin av.b3 on vascular endothelial cells. *Journal of Cellular Physiology* **188**:394-402.

Trikha M, Zhou Z, Nemeth JA, Chen Q, Sharp C, Emmell E, Giles-Komar J and Nakada MT (2004) CNTO 95, a fully human monoclonal antibody that inhibits av integrins, has

antitumor and antiangiogenic activity in vivo. *International Journal of Cancer* **110**:326-335.

Tsou R and Isik FF (2001) Integrin activation is required for VEGF and FGF receptor protein presence on human microvascular endothelial cells. *Molecular and Cellular Biochemistry* **224**:81-89.

Wilder RL (2002) Integrin alpha V beta 3 as a target for treatment of rheumatoid arthritis and related rheumatic diseases. *Annals of the Rheumatic Diseases* **61**:ii96-ii99.

Wilkinson-Berka Jennifer L, Jones D, Taylor G, Jaworski K, Kelly Darren J, Ludbrook Steve B, Willette Robert N, Kumar S and Gilbert Richard E (2006) SB-267268, a nonpeptidic antagonist of alpha(v)beta3 and alpha(v)beta5 integrins, reduces angiogenesis and VEGF expression in a mouse model of retinopathy of prematurity. *Invest Ophthalmol Vis Sci FIELD Full Journal Title:Investigative ophthalmology & visual science* **47**:1600-1605.

Williams R. AM, Baxter H., Forrester J., Kennedy-Martin, T., Girach A. (2004) Epidemiology of diabetic retinopathy and madular oedema: a review. *Eye (London, England)* **18**:963-983.

Witmer AN, van Blijswijk BC, van Noorden CJF, Vrensen GFJM and Schlingemann RO (2004) In vivo angiogenic phenotype of endothelial cells and pericytes induced by vascular endothelial growth factor-A. *Journal of Histochemistry and Cytochemistry* **52**:39-52.

Xu Q, Quam T and Adamis A (2001) Sensitive blood-retina barrier breakdown quantitation using Evans blue. *Invest Ophthalmol Vis Sci* **42**:789-794.

Yasukawa T, Hoffmann S, Eichler W, Friedrichs U, Wang Y-S and Wiedemann P (2004) Inhibition of experimental choroidal neovascularization in rats by an av-integrin antagonist. *Current Eye Research* **28**:359-366.

Yoon K.C. AKY, Lee J.H., Chun B.J., Park S.W., Seo M.S., Park Y.-G., Kim K.K. (2005) Lipid-mediated delivery of brain-specific angiogenesis inhibitor 1 gene reduces corneal neovascularization in a n invivo rabbit model. *Gene Therapy* **12**:617-624.

Zarbin MA (2004) Current concepts in the pathogenesis of age-related macular degeneration. *Archives of Opthalmology* **122**:598-614.

Zhang D, Pier T, McNeel Douglas G, Wilding G and Friedl A (2007) Effects of a monoclonal anti-alphavbeta3 integrin antibody on blood vessels - a pharmacodynamic study. *Invest New Drugs FIELD Full Journal Title:Investigational new drugs* **25**:49-55.

LEGENDS FOR FIGURES

Figure 1. Structure of JNJ-26076713.

Figure 2. A) Inhibition of fetal bovine serum and FGF induced HUVEC migration. The data were normalized to percent of control (Vehicle), which was considered as 100%. ** Statistically different from control ($p < 0.05$, t-test). *** Statistically different from control ($p< 0.001$, t-test).
B) Inhibition of VEGF induced migration. Data was normalized to migration in vitronectin-coated transwells without VEGF stimulation, which was set to 100 % migration. ** Statistically different from VEGF- treated group ($p < 0.05$, t-test). *** Statistically different from VEGF-treated group ($p< 0.001$, t-test).

Figure 3. Inhibition of angiogenesis in the CAM model. CAM tissue directly beneath the filter disk was resected from embryos treated 48 hours prior with JNJ-26076713 and examined under a stereomicroscope. Digital images of CAM sections adjacent to filters were collected and analyzed. The number of vessel branch points contained in a circular region equal to the area of a filter disk were counted for each section. Significantly different from FGF_2 treated CAMs (*** $p< 0.001$, t-test).

Figure 4. Representative images demonstrating inhibition of angiogenesis in the CAM model following exposure to JNJ-26076713 (30X). A) PBS treated control. B) FGF-treated. C) FGF + JNJ-26076713 at 0.1 μg/CAM. D) FGF + JNJ-26076713 at 10 μg/CAM.

Figure 5. Dose–response inhibition of retinal neovascularization with JNJ-26076713 in the mouse OIR model. The efficacy of treatment was calculated as the percent average nuclei per section in the injected eye versus the uninjected eye. The vehicle group was set to 100 % and the treatment group's effects were calculated relative to the vehicle control. JNJ-26076713

significantly inhibited retinal neovascularization at all dose levels (***p < 0.001, ANOVA followed by Tukey's multiple comparison test).

Figure 6. A) Inhibition of retinal vascular permeability in diabetic rats with JNJ-26076713, 60 mg/kg, po, *b.i.d*.. The eyes are enucleated and the retinae are carefully dissected away under an operating microscope. Retinal permeability is expressed as ng Evans Blue/g retina dry weight (Y-axis). This parameter is derived from the amount of Evans Blue extracted from the retina and the dry weight of the retina following at the end of the study following Evans blue perfusion and is indicative of vascular leakage. B) Effect of JNJ-2607613 at 60 mg/kg, po, *b.i.d*. on leukostasis in diabetic rats. NDM = non-diabetic mellitus. DM = diabetic mellitus. * Significantly different from non-diabetic control (p< 0.05, t-test). † Significantly different from diabetic control (P< 0.05, t-test).

JPET Fast Forward. Published on December 14, 2007 as DOI: 10.1124/jpet.107.131656
This article has not been copyedited and formatted. The final version may differ from this version.

Table 1. Inhibition of cell adhesion by JNJ-26076713

Cell	HMVEC	Mouse EC	Rat EC	HT29 ($\alpha_V\beta_6$)	K562 ($\alpha_5\beta_1$)
Matrix	Vitronectin	Vitronectin	Vitronectin	Fibronectin	Fibronectin
IC_{50} (nM)	13.9 ± 0.9	324 ± 164	63 ± 8	100 ± 23	> 50,000

JPET Fast Forward. Published on December 14, 2007 as DOI: 10.1124/jpet.107.131656
This article has not been copyedited and formatted. The final version may differ from this version.

Table 2. Pharmacokinetic parameters in rats following intravenous (IV) and oral dosing (PO)

IV	$t_{½}$ (h)	Cmax (ng/mL)	AUC (h*ng/mL)	Vz (mL/kg)	Cl (mL/min/kg)
Mean	10	45030	13251	1996	2
PO	$t_{½}$ (h)	tmax (min)	Cmax (ng/mL)	AUC (h*ng/mL)	F (%)
Mean	8.2	15	5125	13592	21

$t_{1/2}$ = terminal elimination half life, Cmax = maximal concentration achieved, tmax = time at which maximal concentration was achieved, AUC = area under the curve, V_Z = volume of distribution, Cl = clearance rate, F (%) = percent oral bioavailability.

Table 3. Pharmacokinetic parameters in mice

IV	$t_{½}$ (h)	Cmax (ng/mL)	AUC (h*ng/mL)	Vz (mL/kg)	Cl (mL/min/kg)
Mean	8.3	20400	4664	4752	7
PO	$t_{½}$ (h)	tmax (min)	Cmax (ng/mL)	AUC (h*ng/mL)	F (%)
Mean	4.9	15	1005	3966	17

$t_{1/2}$ = terminal elimination half life, Cmax = maximal concentration achieved, tmax = time at which maximal concentration was achieved, AUC = area under the curve, V_Z = volume of distribution, Cl = clearance rate, F (%) = percent oral bioavailability.

Table 4. Effect of JNJ-26076713 on body weight and blood glucose levels

	Day 1		Day 7		Day 14	
	BW (g)	BG (mg/dl)	BW (g)	BG (mg/dl)	BW (g)	BG (mg/dl)
NDM (-)	217 ± 16	113 ± 5	257 ± 28	103 ± 4	289 ± 22	ND
DM (-)	215 ± 7	357 ± 47	224 ± 19	357 ± 36	239 ± 28	401 ± 58
DM (+)	214 ± 8	369 ± 46	232 ± 14	377 ± 41	245 ± 22	360 ± 76

NDM = non-diabetic mellitus; DM = diabetic mellitus; (-) = vehicle treated; (+) = JNJ-26076713 treated; BW = body weight; BG = blood glucose; ND = not determined

JPET Fast Forward. Published on December 14, 2007 as DOI: 10.1124/jpet.107.131656

Figure 1

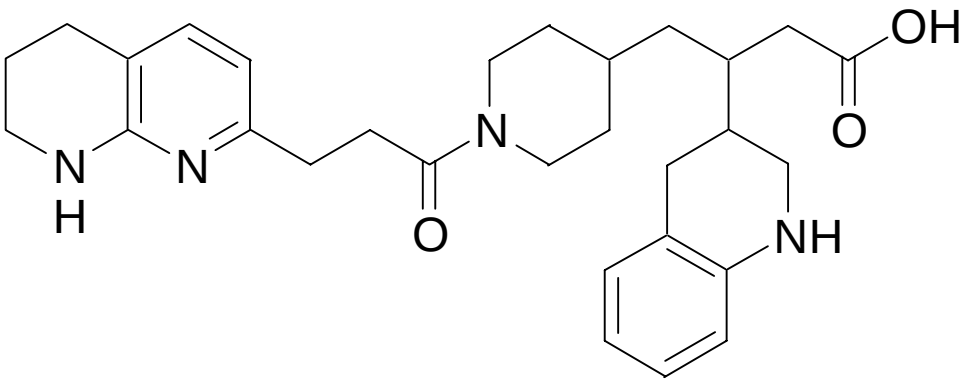

JPET Fast Forward. Published on December 14, 2007 as DOI: 10.1124/jpet.107.131656
This article has not been copyedited and formatted. The final version may differ from this version.

Figure 2

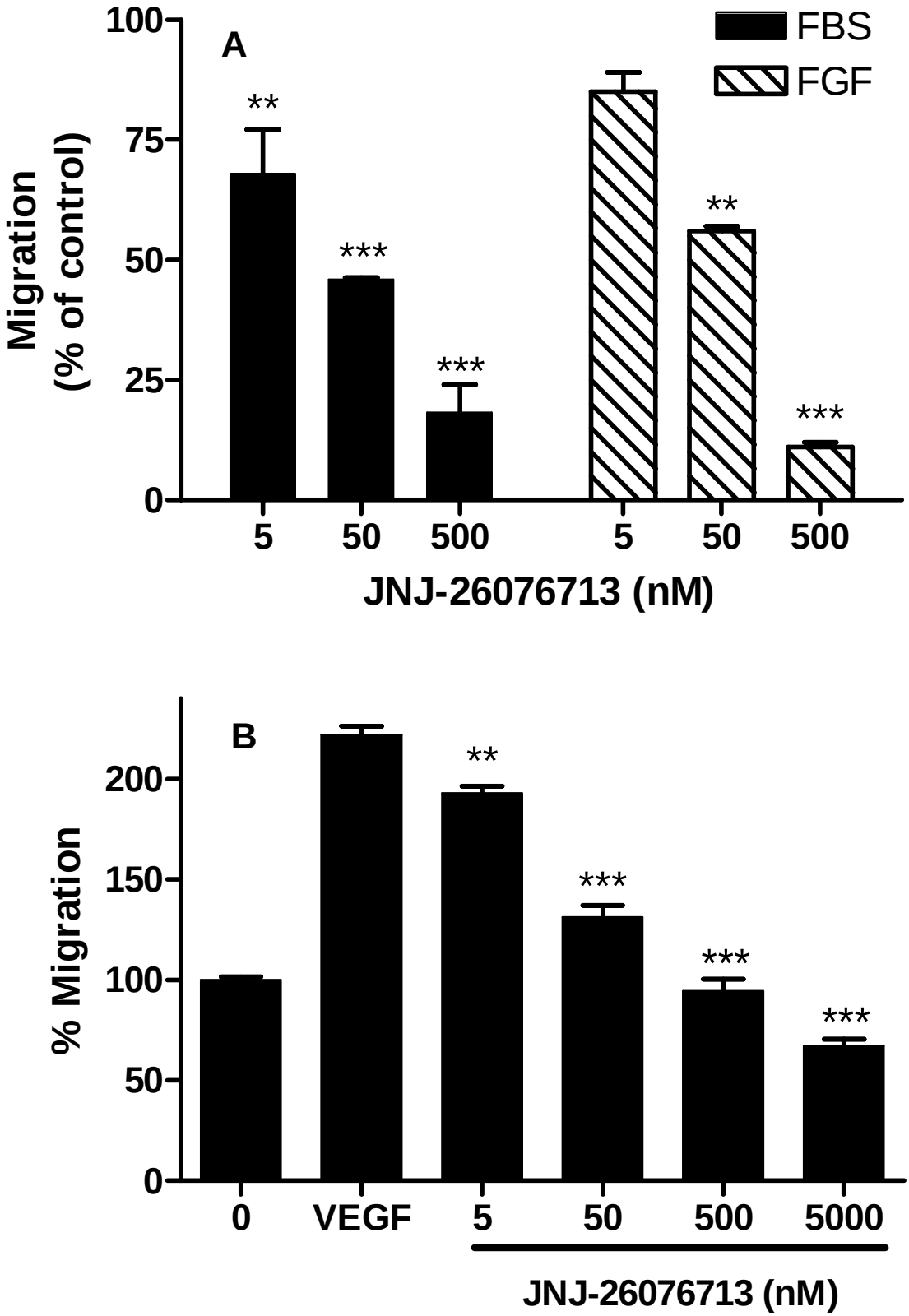

JPET Fast Forward. Published on December 14, 2007 as DOI: 10.1124/jpet.107.131656
This article has not been copyedited and formatted. The final version may differ from this version.

Figure 3

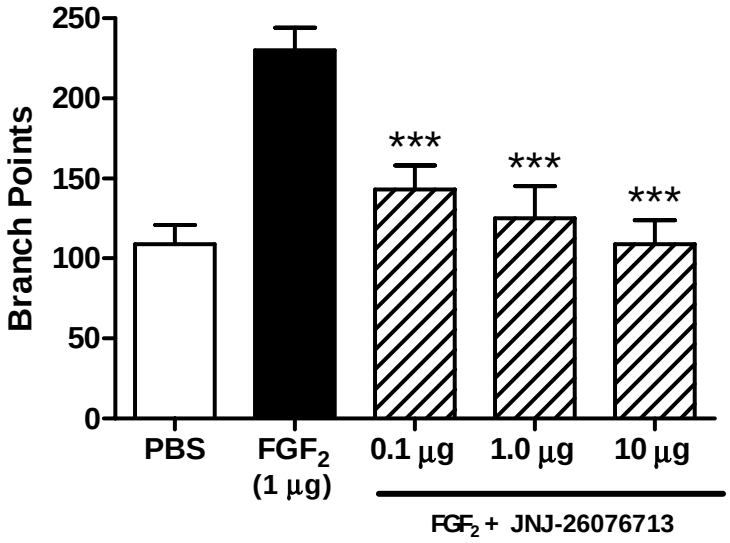

JPET Fast Forward. Published on December 14, 2007 as DOI: 10.1124/jpet.107.131656
This article has not been copyedited and formatted. The final version may differ from this version.

Figure 4

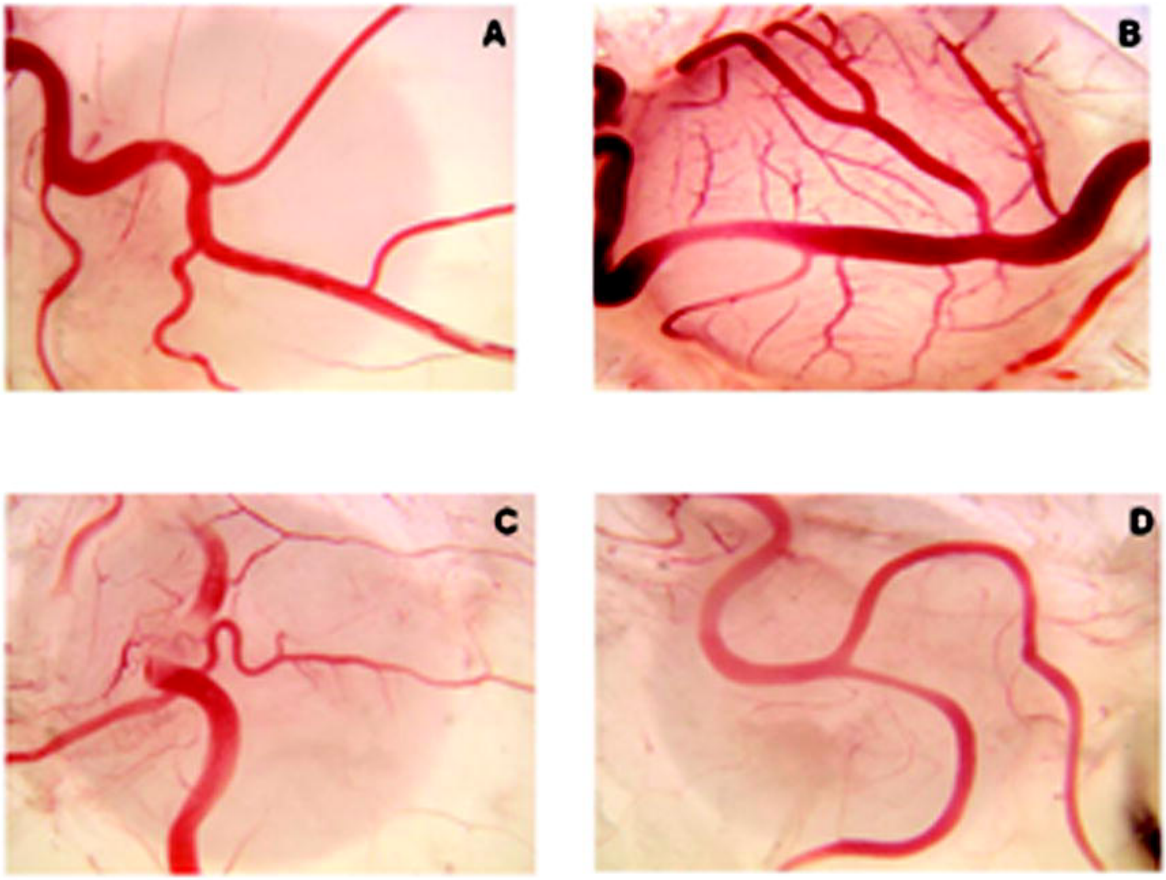

JPET Fast Forward. Published on December 14, 2007 as DOI: 10.1124/jpet.107.131656
This article has not been copyedited and formatted. The final version may differ from this version.

Figure 5

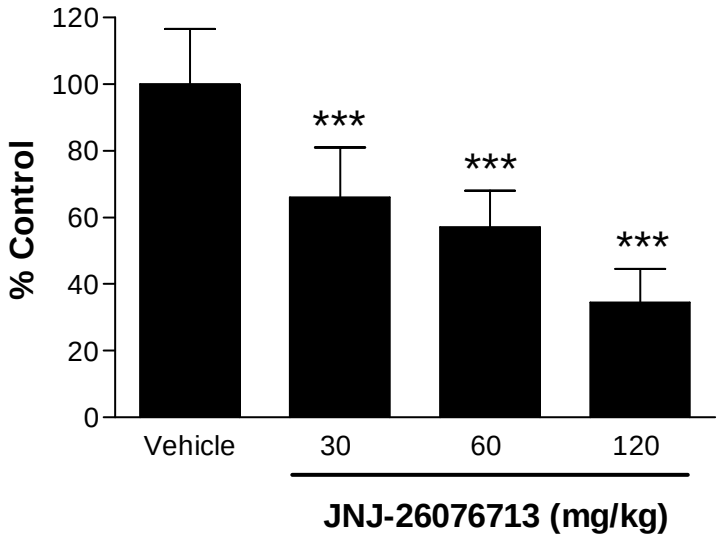

JPET Fast Forward. Published on December 14, 2007 as DOI: 10.1124/jpet.107.131656
This article has not been copyedited and formatted. The final version may differ from this version.

Figure 6